Development of a space-approved vacuum arc thruster

IEPC-2024-286

Presented at the 38th International Electric Propulsion Conference
Pierre Baudis Convention Center • Toulouse, France
June 23-28, 2024

Roman Forster[1], Michal Szulc[2] and Jochen Schein[3]
University of the Bundeswehr Munich, Neubiberg, 85577, Germany

In this work, the development of a vacuum arc thruster (VAT) with corresponding power processing unit (PPU) for the Seamless Radio Access Networks for Internet of Space (SeRANIS) mission is described. The thruster is integrated with the PPU into a package that fulfills the mechanical launch requirements and has passed the vibrational system tests. The PPU is based on an inductive energy storage (IES) design, operates autonomously with safety precautions and provides feedback data on the status of the VAT. The performance of the proposed thruster is evaluated by direct thrust measurements. The expansion and propagation of the plasma plume and the ejected macroparticles are also assessed.

Nomenclature

$\bar{d}$	=	Averaged displacement
g	=	Gravitational constant
I_{sp}	=	Specific impulse
k	=	Spring rate
$\dot{m}_t$	=	Total erosion rate
η	=	Efficiency
P	=	Power
T	=	Thrust
u_i	=	Ion velocity
x_{FA}	=	Distance between force actuator and pivot
x_S	=	Distance between distance sensor and pivot
x_T	=	Distance between thruster and pivot

I.Introduction

In recent years, the demand for propulsion systems for small or micro-satellites is growing due to the increasing usage of such satellites. The vacuum arc thruster (short VAT) is one suitable electric propulsion system for such small satellites. Because of its scalability regarding mass and power consumption, it can even be used as a propulsion system for CubeSats -as small as 1U- where mass and power budget are strictly limited [1–4]. The VAT basically consists of two electrodes separated by an insulator [5,6]. By applying a high electric field between both electrodes, electrons are emitted from the cathode eventually leading to thermal emission and arc spot formation. In addition to the emitted metal vapor from the arc spot, macroparticles are ejected as the surface of the cathode is locally melted [7]. The vapor is ionized and can be observed as expanded plasma plume. The acceleration of the plasma results from the electromagnetic forces due to the discharge current, a high-pressure gradient caused by the sudden explosion of the cathode material, and the momentum transfer between the fast electrons and the slower ions. The accelerated plasma generates a force in the opposite direction to their propagation direction, according to the law of conservation

[1] Ph.D. student, Institute of Plasma Technology, roman.forster@unibw.de.
[2] Ph.D., Institute of Automation and Control, michal.szulc@unibw.de.
[3] Professor, Institute of Plasma Technology, js@unibw.de.

of momentum [8,9] hence producing an accelerating force on the thruster/satellite. Since the eroded cathode material acts as propellant, no additional propellant supply system is required. To initiate the discharge between both electrodes, a sufficiently strong (voltage and current) ignition pulse is necessary, which needs to be provided by the connected power processing unit (short PPU). The PPU can be operated according to various concepts, such as pulse forming networks, capacitive energy storages, inductive energy storages, high voltage sparks or a combination of these [10,11]. However, since the PPU should also have a low mass, the inductive energy storage concept has become established. Such a circuit consists basically of a coil and a semiconductor, similar to an ignition coil in a gas-powered engine, which can be complemented by a capacitor. When a switch is triggered, the energy stored in the coil produces a high voltage peak sufficient to initiate a breakdown between the electrodes [12–14]. A VAT can be operated using ignition modes, with triggerless ignition being the most commonly used. In this mode, the insulator is coated with a conducting layer. The applied voltage is transferred through the resistive layer to the very small insulator-cathode gap whereby an arc can be established using comparatively small initiation voltages [15]. Hence in this case a coil with a lower inductance can be used. As a consequence, the mass of the PPU used is reduced. Inductive energy storages can be operated with supply voltages of less than 24 V, what makes them suitable for microsatellites [5,6].
The SeRANIS satellite mission, which is planned and realized by the University of the Bundeswehr Munich, offers a possibility to test the functionality and performance of a successfully tested laboratory model of a vacuum arc thruster in space. The satellite called Athene-1 is a small satellite with mass of about 300 kg. It will act as a multifunctional laboratory, with more than fifteen experiments with a total mass of circa 90 kg to be mounted on the satellite. This project can serve as next evaluation step for the research group of space at the University of the Bundeswehr Munich, which works in many different fields regarding space application [16,17].

II.Design of thruster and power processing unit

The thruster with its tailored power processing unit was developed according to the given requirements of the platform of the Athene-1 satellite. The experiment is connected to the unregulated voltage bus of the satellite, the values of which are ranging between 26 V and 32.8 V. A power supply and control unit (short PSCU) generates a supply voltage of 24 V at 3 A for the PPU. The unit also initiates the discharge by triggering the PPU, evaluates the output data of the PPU and ensures communication with the satellite platform.

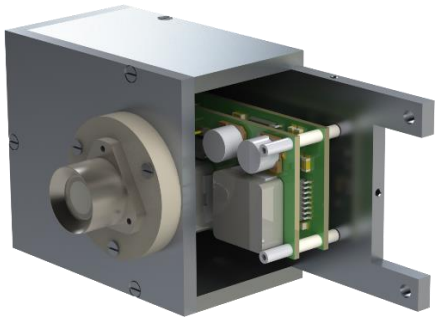

Figure 1: VAT with aluminum housing as sectional view and PPU.

The thruster consists of two cylindrical electrodes separated by an insulator. The anode is made of stainless steel, the cathode of titanium and the insulator of PEEK. The thruster and the PPU are mounted in an aluminum housing measuring 98 mm x 58 mm x 39 mm as shown in Fig. 1. The entire VAT package weighs about 311 g. The thruster is designed to operate in the triggerless mode. When the thruster is triggered, the initial discharge current evaporates this layer, but part of the following metal plasma jet from the cathode is redeposited on the surface of the insulator and the conductive layer is restored. Triggerless operation depends on several conditions, such as for example the pulse energy, and is only reliable for a certain amount of pulses, and is therefore the main limiting factor for the operating time of a VAT. The PPU used is based on the principle of an inductive energy storage with a capacitor and was optimized to extend the operating time of triggerless mode. As specified in the operation sequence of the experiments during the mission, the VAT will only operate in defined timeslots when no other experiment is running. When the PPU is triggered by the PSCU, a capacitor is charged until a predefined value is reached. Then, the power bus is disconnected to prevent any unwanted electrical interference from being fed back into the PSCU or satellite's supply bus. At the same time, a signal is generated to charge the inductor. After the inductor is charged, the IGBT is switched off, resulting in the desired voltage peak to initiate a discharge of the VAT. The ignition process runs automatically. In case of a fault, a watchdog circuit resets the PPU. Furthermore, the PPU is also able to diagnose the condition of the thruster head. The two monitored parameters are the voltage at the capacitor and the discharge current flowing through the thruster. Both values are converted into a logic signal and evaluated by the PSCU.

III.Experimental set-up

A. Thrust and performance

A thrust balance system made by FOTEC GmbH, Wiener Neustadt, Austria, capable of measuring thrusts in the range of up to one micronewton, was used to determine the thrust generated by the VAT. The balance system is shown schematically in Fig. 2.

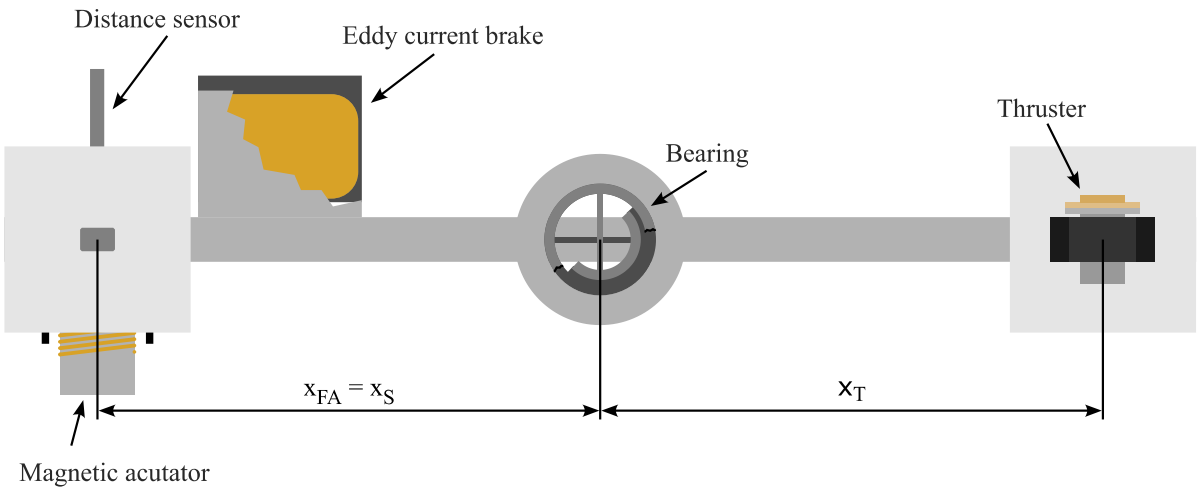

Figure 2: Scheme of the thrust balance system.

The system consists of a beam suspended by two stainless-steel spring bearings. A table at each end of the beam is used for mounting the thruster and a corresponding counterweight on the other side. The deflection of the beam is detected by a high precision optical distance sensor. A calibrated magnetic feedback coil (force actuator) is responsible for maintaining the resting position of the beam. Therefore, the thrust can be determined by measuring the displacement of the beam or by determining the force applied by the actuator to compensate the thrust generated by the VAT. The electrical connection of the thruster is realized by electrical feed-throughs, which are capable of conducting high-current and high-voltage signals without exerting any possible force on the beam.

Using the small angle approximation, the thrust generated by the VAT can be calculated via displacement as with sensor distance is equal to thruster distance:

$$T = \frac{k}{x_T^2}\bar{d} \tag{1}$$

The variable x_T describes the distance of the thruster to the pivot point, k stands for the spring rate of the bearings and $\bar{d}$ describes the averaged displacement measured by the optical sensor.

Besides the thrust, the specific impulse is also an important parameter for electric propulsion systems. It indicates how efficient the propellant is utilized. Specific impulse is calculated as:

$$I_{sp} = \frac{T}{\dot{m_t} g} \tag{2}$$

For the calculation of the specific impulse the total mass flow $\dot{m}_t$ and the constant of gravitation are needed.

The efficiency of the VAT is defined as the ratio of the generated thrust to input power, which is equal to the discharge power. Therefore, the efficiency can be expressed as:

$$\eta = \frac{T^2}{2\dot{m_t} P} \tag{3}$$

The thrust-to-power ratio describes another specific parameter for a propulsion system and is computed with the following formula with u_i as ion exit velocity:

$$\frac{T}{P} = \frac{2\eta}{u_i} \tag{4}$$

B. Plume analysis

Since the VAT not only emits metal vapor, but also macroparticles that may deposit on sensitive parts of the satellite or other experiments, such as antennas or optical systems, it is necessary to analyze the plume expansion of the VAT. To detect the propagation angle of the plume, nine microscope slides were placed in a semi-circle with the VAT in the center of the circle, as depicted in Fig. 3.

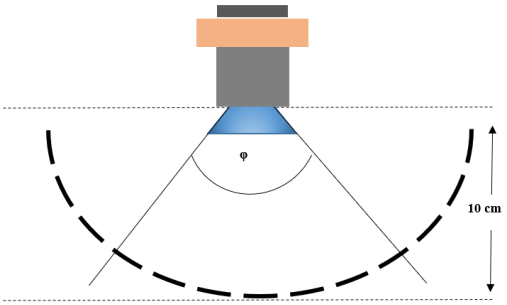

Figure 3: Scheme of plume expansion detection.

The radius of the semi-circle was ten centimeters, measured from the center of the anode. The VAT performed twenty thousand pulses and the radiation angle was measured manually by investigating the coating of each of the slides.

To further investigate the propagation angle, the plasma plume of the thruster was observed simultaneously from six directions of view using an intensified camera. A Dicam C1 manufactured by Excelitas PCO GmbH, Kehlheim, Germany, was used. Assuming that the expanding plasma is optically thin, the six directions of view can be used to calculate a rough tomographic reconstruction of the plume.

As shown in Fig. 4, the six mirrors were arranged cylindrically in 30-degree increments on a metal carrier plate with an offset of 15° to the horizontal plane. All deflection mirrors were manufactured by Edmund Optics Inc., Barrington, NJ, USA. Based on the radon transform of a two-dimensional function $f(x, y)$, the inverse Radon transform of the six recorded projections originating from the six deflection mirrors was computed. Then, the algebraic reconstruction technique was used to reconstruct the expanding plasma from the projections.

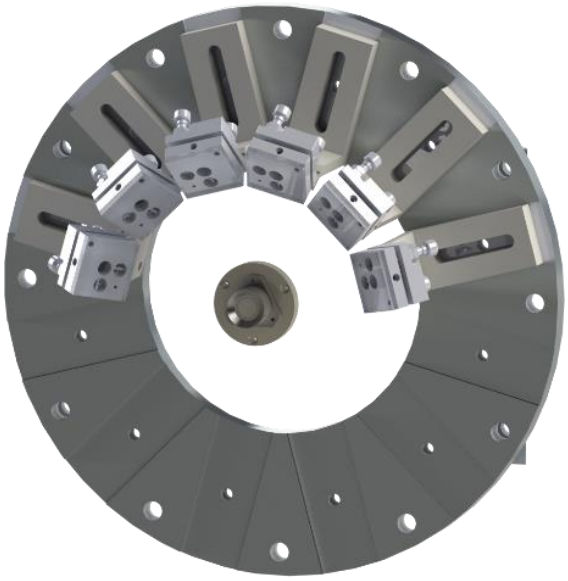

Figure 4: Arrangement of the mirrors to observe the thruster from six directions of view with the VAT placed in the center.

C. Vibrational Tests

Mechanical tests were performed to check whether the experiment can withstand the stresses that occur during the launch of the mission. This step included sinusoidal and random vibration tests. A model check was done before and after these tests to evaluate the natural frequency of the experiment. According to the mission requirements, the first natural frequency has to be greater than 500 Hz. The required values that the experiment has to withstand in the sinusoidal vibration test are summarized in Table 1, while the values for the random vibration test in Table 2. All tests were performed for each axis.

Table 1: Requirements for sine vibration tests.

Frequency [Hz]	Acceleration [g]
5	2
15	20
40	20
50	15
150	15

Table 2: Requirements for random vibration tests.

Frequency [Hz]	Acceleration [g]
20	0.1
50	0.8
250	0.8
400	0.24
1000	0.24
2000	0.125
GRMS	23.5

All mechanical vibrational tests were performed by a SD-5280-13 series vibration test system, manufactured by Spectral Dynamics Inc., San Jose, CA, USA. The experiment was mounted on the test rig in the same way as it will be mounted on the satellite. For each test, two position sensors were attached to the experiment and one control sensor to the adapter plate. The control sensor monitors the reference vibration, while the position sensors record the vibration of the experiment. The positioning of the sensors changed depending on the vibration direction being investigated.

The setup of the vibrational test for the z-axis, which points out of the page, is shown schematically in Fig. 5. The blue polygon indicates the control sensor, which was mounted on the adapter plate of the system. The first acceleration sensor was placed in the left bottom corner of the experiment, which can be recognized by the orange marking. This point is as close as possible to the instrumental reference point for satellite mounting. The second acceleration sensor was positioned close to the thruster head, marked as green triangle in Fig. 5.

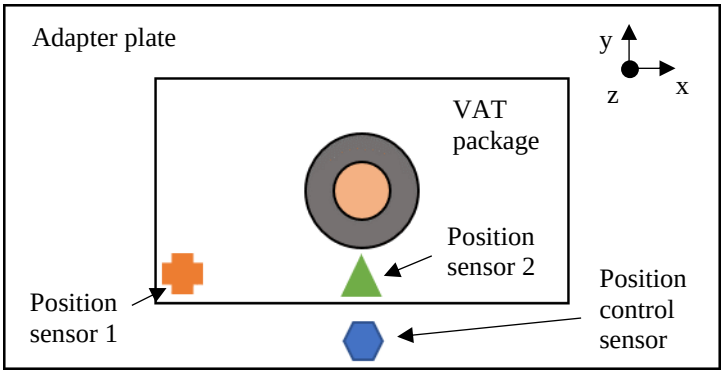

Figure 5: Scheme and sensor arrangement for vibrational tests for the z-axis.

IV.Experimental results

A. Thrust and performance

The thrust of the VAT was determined by measuring the displacement of the balance beam with the force actuator switched off. The ambient pressure during the measurement was about 5 x 10^{-4} mbar at room temperature. The duration of the measurements was set to three minutes, with the first and the third minutes being recorded to determine the drift of the thrust measurement system. The thruster was pulsed for one minute at an operating frequency of 10 Hz.

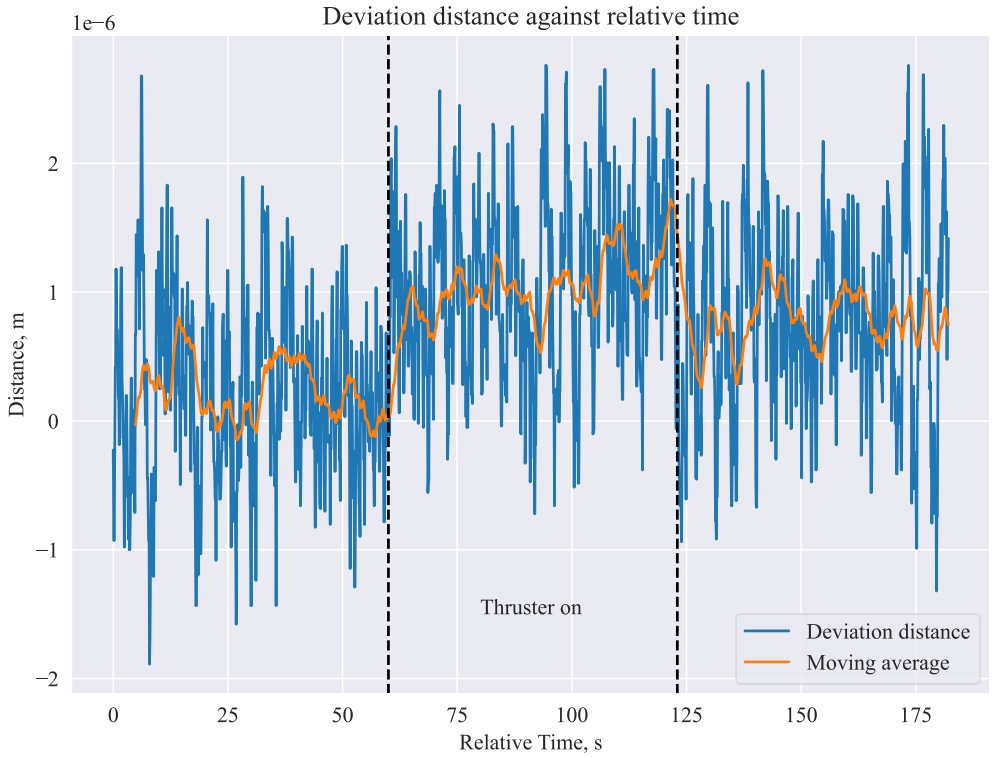

Figure 6: Thrust measurement via displacement.

Figure 6 shows an exemplary measurement recorded in displacement mode. The deviation distance of the optical sensor is marked in blue, while the moving average of the signal is marked in orange. The thruster operated in the time between the two black and dashed vertical lines. After removing the determined drift, an averaged displacement of 0.553 µm was estimated, which yields a thrust of 1.26 µN according to eq. 1. The specific impulse was calculated using an erosion rate of 30 µg/C from the literature and results in 1129 s [18]. The efficiency amounted to 1.94 % and the thrust to power ratio was 3.5 µN/W.

B. Plume analysis

The evaluation of the propagation angle of the plasma plume after twenty thousand discharge pulses resulted in an angle of about 150°. The angle was measured manually and can be regarded as qualitative diagnostic.

Additionally, the plasma plume was investigated optically by observing the discharge from six directions of view. Based on the projections, a simplified 3d-model of the plasma plume was computed.

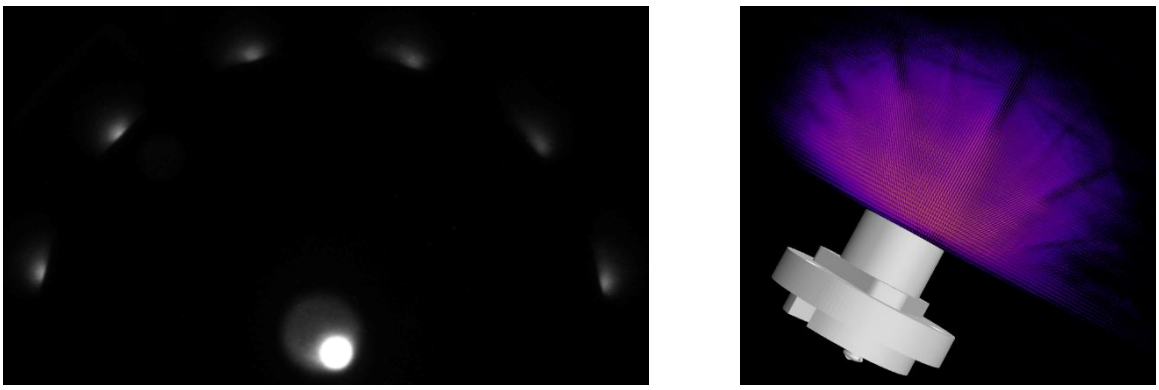

Figure 7: Tomographic reconstruction of the plasma plume; Left: Recorded image of the plasma plume and the six directions of view; Right: Rough 3D reconstruction based on the left image with VAT.

Figure 7 shows the optical measurement of the VAT plasma plume. The image on the left-hand side depicts the recorded camera image, in which the ignited VAT can be seen in the center with the six directions of view around it. The image was captured 500 µs after the ignition with an exposure time of 1.5 µs. After calculations, the reconstructions can be stacked to a 3d-model of the observed object. The image on the right-hand side in Fig. 7 shows the reconstructed plasma plume. A 3d-model of the thruster is additionally displayed for a better visualization. The reconstructed 3d-model indicates that the propagation angle of the plume is smaller than 180°, which is consistent with the results observed on the coated microscopic slides.

C. Vibrational tests

The first step of the vibrational test was to determine the natural frequency of the experiment, followed by the sine and random vibrational tests for each axis. At the beginning and after each sine and random test, the natural frequency was evaluated to check whether any changes are noticeable.

The accelerations measured by the sensors are plotted in Fig. 8 for the natural frequency measurement with respect to the z-axis. The curves of both acceleration sensors, sensor 1 and 2, indicate that the first natural frequency exceeds 2000 Hz. As a consequence, the requirements regarding the stiffness of the experiment are fulfilled. Besides this, no mechanical damage was found in the experiment after performing the sine and random vibrational tests and the function of the VAT was not affected by the tests.

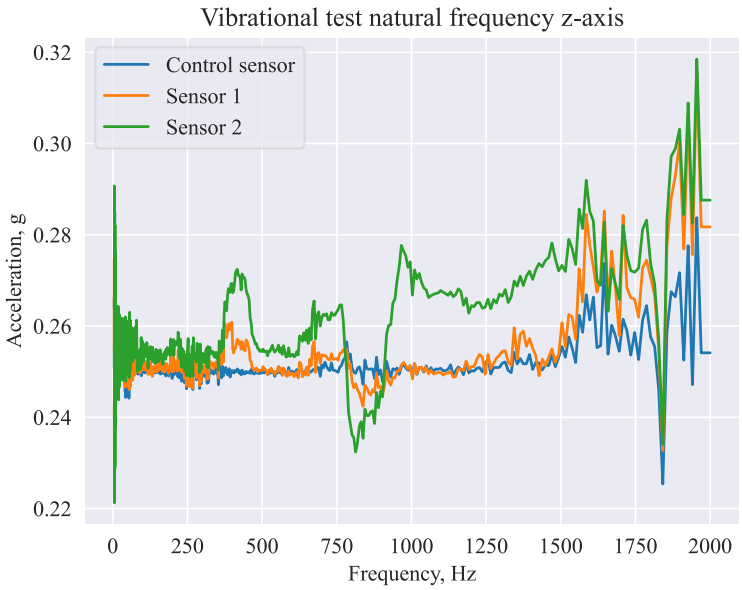

Figure 8: Recorded measurement for the natural frequency.

V.Discussion and outlook

This paper presents an intermediate status of the development of a VAT model for the SeRANIS small satellite mission. The thruster system was developed in accordance with the requirements of the mission. The PPU, which is based on the concept of inductive energy storage, operates with a supply voltage of 24 V at 3 A. The generation of pulses is automated and runs according to a defined sequence that is started by an incoming trigger signal. This sequence includes several measures to minimize possible interferences and detect faulty conditions. Among other measures, the trigger input is disabled as soon as the PPU has received an input signal to prevent multiple triggering. The PPU is separated from the power bus of the satellite during the ignition to reduce possible disturbances. During operation the capacitor voltage as well as the discharge current of the VAT are monitored to estimate the condition and wear of the thruster. The developed thruster package generates a mean thrust of 1.26 µN and a mean specific impulse of 1129 s. This leads to an efficiency of 1.94 % and a thrust-to-power ratio of 3.5 µN/W.

The propagation of the plasma plume generated by the discharge was investigated with two methods: by placing witness plates around the VAT and analyzing the coating of these targets, and optically by observing the plume from six directions of view and subsequently calculating a rough tomographic reconstruction. Both methods indicated similar results that the radiation angle of the plasma is less than 180°. The first method was also used to estimate the expansion of emitted macroparticles. These investigations were necessary for the platform provider to evaluate the arrangement of the experiments on the Athene-1 satellite.

Further requirements that have to be fulfilled according to the mission requirements concern mechanical stability and interface. These include a mass limit of 312 g for the VAT with the corresponding PPU. Besides this, the mechanical stiffness of the model has to have a first natural frequency of over 500 Hz. To verify this requirement, vibration tests were carried out with sine and random frequency excitation. The developed thruster package fulfills the mass limitation and the requirements for the first natural frequency, which is above 2000 Hz. The package is furthermore considered to be mechanically stable, as it showed no mechanical damages or impairment of functionality after the vibration tests.

Nonetheless, the development is not yet complete. Future work includes the required thermal and EMI tests. In the prior, the functionality of the thruster and the PPU has to be demonstrated during various thermal cycles. The latter will be carried out to check conducted and radiated emissions and to assess susceptibility to interference.

VI.Conclusion

In this paper, a VAT with bespoke PPU was developed in accordance with the mission requirements for the Athene-1 satellite. The performance of the thruster was evaluated experimentally. Then, several tests were performed to verify that the proposed design meets the requirements. The propagation of the plasma plume and the ejected macroparticles were investigated. It could be shown that the mechanical requirements are fulfilled as the presented system passed the vibration tests.

Acknowledgments

This work was supported by SeRANIS (dtec.bw).

References

1. Kronhaus, I.; Schilling, K.; Pietzka, M.; Schein, J. Simple Orbit and Attitude Control Using Vacuum Arc Thrusters for Picosatellites. *Journal of Spacecraft and Rockets* **2014**, *51*, 2008–2015, doi:10.2514/1.A32796.
2. J. Schein; A. Gerhan; Filip Rysanek; M. Krishnan. 1 Vacuum Arc Thruster for CubeSat Propulsion **2003**.
3. Keidar, M.; Zhuang, T.; Shashurin, A.; Teel, G.; Chiu, D.; Lukas, J.; Haque, S.; Brieda, L. Electric propulsion for small satellites. *Plasma Phys. Control. Fusion* **2015**, *57*, 14005, doi:10.1088/0741-3335/57/1/014005.
4. Kolbeck, J.; Anders, A.; Beilis, I.I.; Keidar, M. Micro-propulsion based on vacuum arcs. *J. Appl. Phys.* **2019**, *125*, doi:10.1063/1.5081096.
5. Filip Rysanek; John William Hartmann; Jochen Schein; Robert Binder. *Microvacuum arc thruster design for a CubeSat class satellite*, 2002.
6. Li, Y.-H.; Pan, J.-Y.; Herdrich, G. Design and demonstration of micro-scale vacuum cathode arc thruster with inductive energy storage circuit. *Acta Astronautica* **2020**, *172*, 33–46, doi:10.1016/j.actaastro.2020.03.012.
7. Beilis, I. Vacuum Arc Ignition. Electrical Breakdown. *Plasma and Spot Phenomena in Electrical Arcs* **2020**, *113*, 143–164, doi:10.1007/978-3-030-44747-2_6.

8. Rysanek, F.; Burton, R. Acceleration Mechanisms in a Vacuum Arc Thruster. In *33rd International Electric Propulsion Conference*, The George Washington University, Washington, D.C., USA, 6-10 October, 2013, ISBN 978-1-62410-098-7.
9. Beilis, I.I. Physics of Cathode Phenomena in a Vacuum Arc With Respect to a Plasma Thruster Application. *IEEE Trans. Plasma Sci.* **2015**, *43*, 165–172, doi:10.1109/TPS.2014.2308929.
10. Kühn, M.; Schein, J. Development of a High-Reliability Vacuum Arc Thruster System. *Journal of Propulsion and Power* **2022**, *38*, 752–758, doi:10.2514/1.B38202.
11. J. Lun. Development of a vacuum arc thruster for nanosatellite propulsion **2009**.
12. Bai, S.; Wang, N.; Xie, K.; Miao, L.; Xia, Q. Performance model of vacuum arc thruster with inductive energy storage circuit. *Acta Astronautica* **2021**, *186*, 426–437, doi:10.1016/j.actaastro.2021.06.008.
13. Jochen Schein; Mahadevan Krishnan; Robert Shotwell; John Ziemer. Vacuum Arc Thruster for Optical Communications Mission. In *33rd International Electric Propulsion Conference*, The George Washington University, Washington, D.C., USA, 6-10 October, 2013, ISBN 978-1-62410-098-7.
14. Schein, J.; Qi, N.; Binder, R.; Krishnan, M.; Ziemer, J.K.; Polk, J.E.; Anders, A. Inductive energy storage driven vacuum arc thruster. *Rev. Sci. Instrum.* **2002**, *73*, 925–927, doi:10.1063/1.1428784.
15. Anders, A.; Brown, I.G.; MacGill, R.A.; Dickinson, M.R. `Triggerless' triggering of vacuum arcs. *J. Phys. D: Appl. Phys.* **1998**, *31*, 584–587, doi:10.1088/0022-3727/31/5/015.
16. Artur Kinzel; Johannes Bachmann; Rishi Jaiswal; Manohar Karnal; Andreas Knopp. Seamless Radio Access Network for Internet of Space (SeRANIS): New Space Mission for Research, Development, and In-Orbit Demonstration of Cutting-Edge Technologies. In *Space for @ll.* 73rd International Astronautical Congress (IAC), Paris, France, 18-22 September; International Astronautical Congress, Ed., 2022.
17. Johannes Bachmann; Artur Kinzel; Francesco Porcelli; Alexander Schmidt; Andreas Knopp. SeRANIS: In-Orbit-Demonstration von Spitzentechnologie auf einem Kleinsatelliten. In *"Luft- und Raumfahrt - gemeinsam forschen und nachhaltig gestalten".* DLRK Deutscher Luft- und Raumfahrtkongress, Dresden, Germany, 27-29 September; Deutsche Gesellschaft für Luft- und Raumfahrt, Ed., 2022.
18. Polk, J.E.; Sekerak, M.J.; Ziemer, J.K.; Schein, J.; Qi, N.; Anders, A. A Theoretical Analysis of Vacuum Arc Thruster and Vacuum Arc Ion Thruster Performance. *IEEE Trans. Plasma Sci.* **2008**, *36*, 2167–2179, doi:10.1109/TPS.2008.2004374.